

FIELD DISTRIBUTIONS WITHIN A RECTANGULAR CAVITY WITH VEHICLE-LIKE FEATURES

Hui Zhang, Lester Low, Jon Rigelsford and Richard Langley

The University of Sheffield
Department of Electronics and Electrical Engineering
Mappin Street, Sheffield, United Kingdom, S1 3J, UK.
Email: R.J.Langley@shef.ac.uk

Abstract

A simple model vehicle cabin was constructed to investigate 3D field distributions generated by an on-board transmitter within a large metal cavity. Simulations were found to be in good agreement with internal field measurements acquired using a low disturbance automated probe positioner at 870 MHz. Results show vehicle furnishings, in particular the metallic components, change field distribution within the cavity and should be included for electromagnetic modelling and field exposure assessments. The study enhances understanding of complex field behavior within a vehicle. The results (e.g. E-field hotspots) can be used to optimize placement locations of on-board transmitters and introduce field mitigation techniques in appropriate locations.

1. Introduction

Modern automotive vehicles incorporate numerous electronic devices to provide communication services and an intelligent environment for the driver. Devices such as mobile telephones, Bluetooth transmitters, tyre pressure monitoring systems and many other wireless transmitters are increasingly being installed within vehicles. Optimizing the performance of transmitters and at the same time ensuring compliance to EMC and radiation safety standards [1] is a challenging task for the automotive engineer. Furthermore, the presence of the vehicle body and dielectric furnishings significantly alters the electric field distribution within a vehicle [2]-[3]. Hence a broader understanding of the field behavior is needed. Earlier studies have reported external 2D (2-Dimensional) field studies from a Terrestrial Trunk Radio (TETRA) transmitter and 1D field radiation levels due to a mobile transmitter within and outside the vehicle [4] – [6]. Field distributions within an empty vehicle cabin due to a micro-strip patch antenna have been described using a scaled vehicle model in [7]. Due to measurement equipment and positioning errors within a vehicle, it is rather difficult to obtain average field magnitude and compare simulation results with experimental results using the limited data points obtained from 1D or 2D measurements [8]. A 3D data set will provide more data points and enable a clearer picture of the field distribution within a vehicle cabin loaded with furnishings. Currently, there is little published literature that describes internal field distributions due to on-board transmitters within a vehicle cabin with furnishings included. This study is important as the vehicle cabin is a resonant cavity with a complex propagation environment [9]. It is highly reflective and can cause spatial field variations. Rather than use an extremely complex vehicle cabin in this project we chose to use a well defined rectangular cavity, of similar volume to that of a medium size car but with well defined dimensions and internal fittings. In this paper, we compare the internal field distributions at 870 MHz of a model vehicle cabin with furnishings to one without. The study involves both calculation of the internal electromagnetic fields and verification of the

simulations with measured experimental data. 3D measurements and simulations were carried out and these are presented as 2D cuts for clarity as explained later. The empty cavity provides a starting point for the study, followed by the introduction of a seat frame (the soft furnishing has relatively little impact), a steering wheel and column and a dielectric dashboard construction. This study is extremely important as confidence in electromagnetic field simulation in complex environments is imperative for automotive and aerospace manufacturers where long design and testing times need to be reduced [10]. The internal fields within the cavity have been computed using two software simulation packages, CST Microwave Studio based on time domain techniques and FEKO which has a method of moments core. The transient solver in CST Microwave Studio was used with a broadband frequency sweep setting. Single frequency field distributions were computed using the Multi-level fast Multi-pole (MLFMM) solver in FEKO. The two different solvers provide different convergence times depending on how the cavity was loaded, e.g. FEKO simulation times increases with inclusion of bulk dielectric materials such as seat foam.

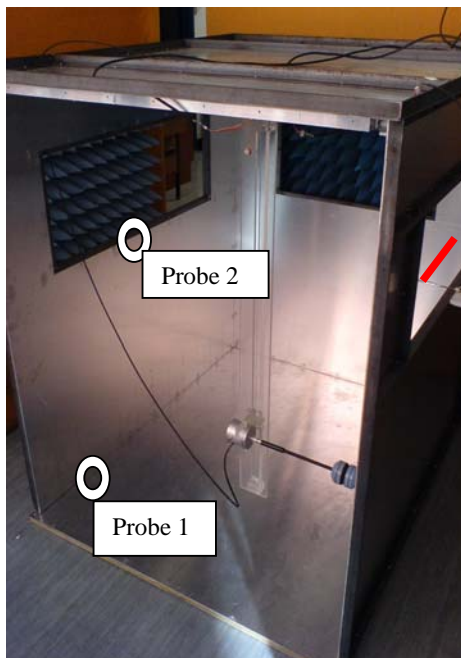


Fig. 1 Simple metal cavity with open window apertures
 Z-direction movement arm shown with field probe attached
 Source antenna shown in red - level with aperture on RHS
 Circles show field probe positions

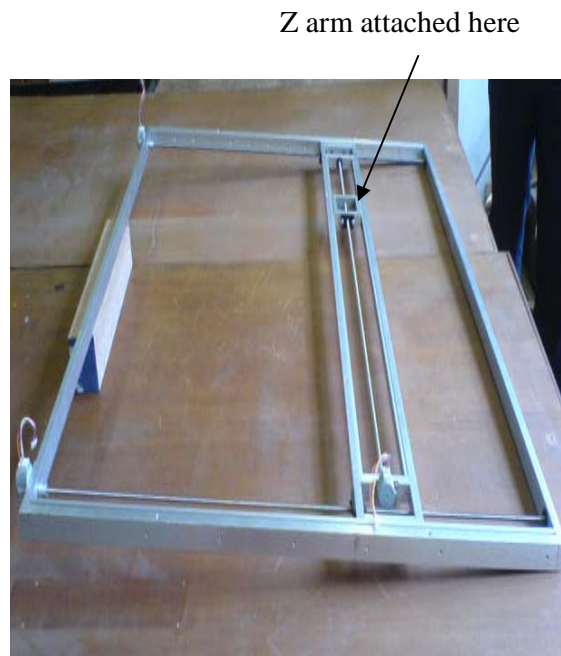


Fig. 2 XY direction scanning frame
 Positioned at top of cavity in Fig. 1

2. Cabin model and field measurement probe positioner

The vehicle cabin model is a rectangular cavity made out of aluminium sheets, bolted and riveted together. Windows are represented by simple apertures. The cavity is shown in Fig. 1 and measured 1200mm x 1000mm x 1200 mm high, the end wall has been removed for clarity. The cavity is well defined electromagnetically. Simple internal furnishings were added to the cavity as described later. The simplicity of the model allows a detailed electromagnetic analysis without the very complex detail of a vehicle so that a fundamental understanding and evaluation of the fields can be undertaken. The internal fields within the cavity have been computed using the two software simulation packages, CST Microwave Studio and FEKO.

Field distributions in the cavity volume are mapped using a low disturbance field probe positioner developed within The University of Sheffield. Fig.1 shows the probe attached to the perspex scanning Z-arm in the cavity. For sufficient structure integrity, the main scanning frame was constructed out of metal to support the moving mechanisms and the free field probe used for field acquisition. Fig.2 shows the metal scanning frame to which the Z-arm is attached. It measures 1100mm x 900mm from the outside edges and controls movement in the XY directions. It was constructed from 22mm metal tubing and has a plastic Z arm which holds the electromagnetic probe. The holder required to support the Z-positioner measures about 75 mm x 120mm and can be seen in Fig.2. For precise positional control and to minimise field disturbance, small stepper motors measuring 30mm in diameter were used to rotate thin metal screws of specific pitch. The XY frame was bolted to the top (roof) of the cavity in Fig. 1 giving minimal interference with the fields in the cavity. The height of the probe within the cavity can be varied with the z-arm positioner. It measures 1000mm in length and is made out of Perspex, a low loss and low reflectivity material introducing minimum disturbance to the cavity fields that are to be measured. The probe positioner can be controlled to within 0.1 mm resolution on any axis of movement.

An IndexSar isotropic air probe (IXP-60) was used to acquire field measurement data within the cavity. An optical fibre feeds the data from the probe to a computer where raw field data is processed and logged. The probe was calibrated at the 900 MHz and 1800 MHz bands and calibration factors at these two frequencies were provided by IndexSAR. The input power for all measurements was 0.3 W into the dipole.

3. Measurements in an empty cavity

Measurements were carried out in the empty cavity for comparison with simulated results and to assess the level of field perturbation introduced by the scanning frame in the cavity. Measurement uncertainties are due to probe positioning errors (+/- 1mm) and cable losses which were corrected. Two assessment methods to gauge the affect of the scanning components have been used.

One method measured the transmission from one antenna to another as a function of frequency. Two results are shown in Fig.3 and Fig.4 which compare the transmission parameter S_{21} of an empty cavity with that of the cavity with the scanning frame mounted in the roof. The transmitting antenna was a horizontal dipole positioned 10 cm inside the cavity and level with the bottom centre of the window. A horizontal monopole field probe was

placed at the points marked by the white discs in Photo 1 to sample the signal at these two positions in the cavity. Fig.3 shows measurements taken at probe position 1 where the field probe was placed 20 cm from the opposite cavity wall to the dipole and directly level with the dipole source. Fig.4 shows measurements taken at probe position 2 which was near the lower base corner 20 cm from each wall. The Z-arm and other parts remain stationary throughout the measurement. Cavity resonance modes can be identified by comparing the two plots. At the lower frequencies from 800 MHz to 1200 MHz amplitude variations are more apparent for the probe at position 1, Fig.3a, when the scanning frame was introduced rather than position 2, Fig.4a. At the higher frequencies, Fig.3b and Fig.4b, amplitude variation occurs for both probe positions indicating more disturbance of the field at these frequencies. However the majority of the resonance peaks and troughs remain in the same position on the frequency axis across both frequency ranges. This indicates that although field levels will vary when the scanning frame is inserted the field mode profile will not change significantly particularly at the lower frequencies around 900 MHz.

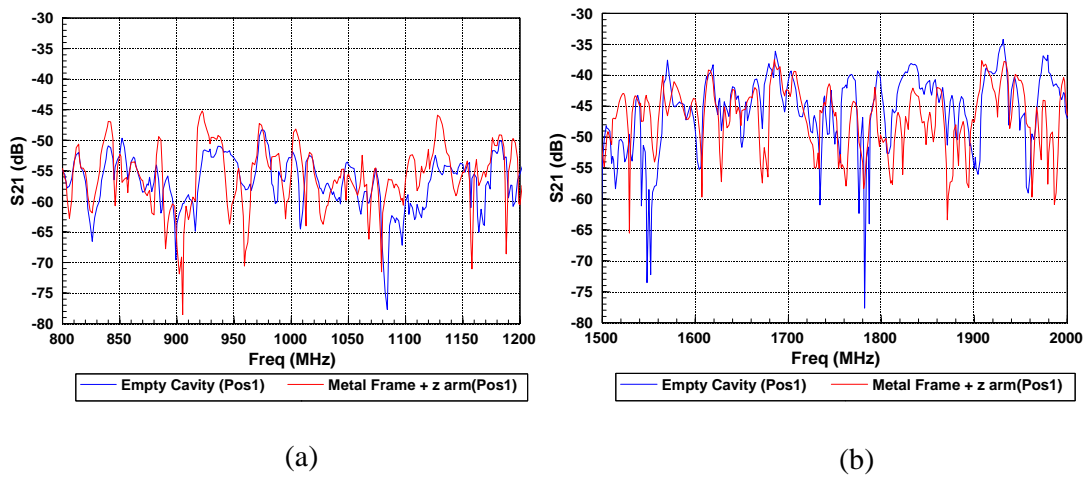


Fig. 3 Measured comparison of S_{21} for empty cavity and with scanning frame mounted at probe position 1

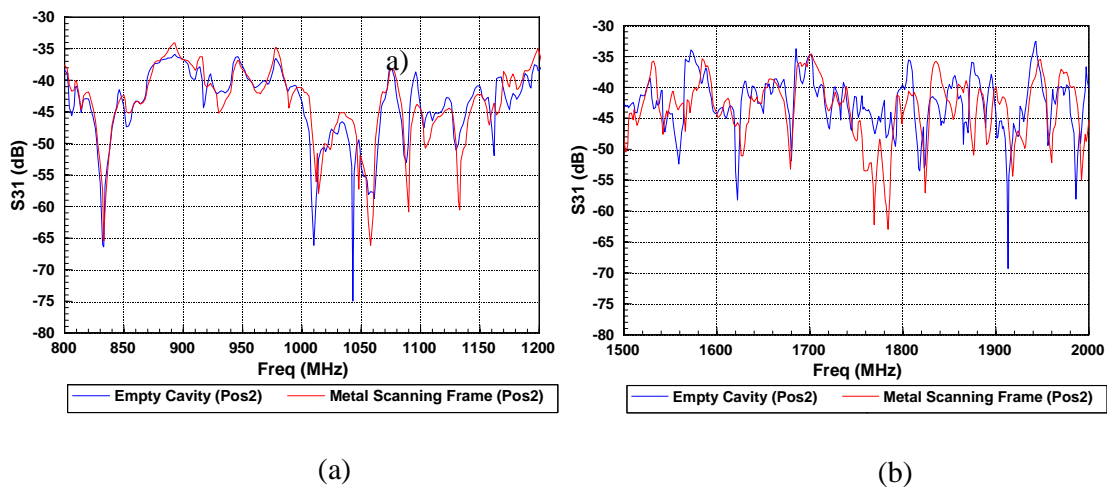


Fig. 4 Measured comparison of S_{21} for empty cavity and with scanning frame mounted at probe position 2

For the second disturbance method a number of cavity simulations were carried out using both CST MWS and FEKO. These simulations showed that each gave very similar field mode results, although the field amplitudes predicted by FEKO were slightly higher than those calculated using CST. Table 1 shows the peak field amplitudes for each simulation package and measurement. The results from CST were in better agreement with measurements than FEKO and this paper concentrates on CST simulation results. A convergence study using uniform mesh for the entire geometry has been conducted using both simulators. A $\lambda/12$ mesh was used for FEKO and a $\lambda/20$ mesh was use for CST MWS.

| | FEKO | CST MWS | Measured |
|------------|------------|------------|------------|
| Plane-95cm | 23.5 dBV/m | 22.6 dBV/m | 20.4 dBV/m |
| Plane-65cm | 23.6 dBV/m | 20.1 dBV/m | 20.2 dBV/m |
| Plane-35cm | 23.8 dBV/m | 20.3 dBV/m | 21.6 dBV/m |

Table 1: Comparison of maximum field levels in the empty cavity.

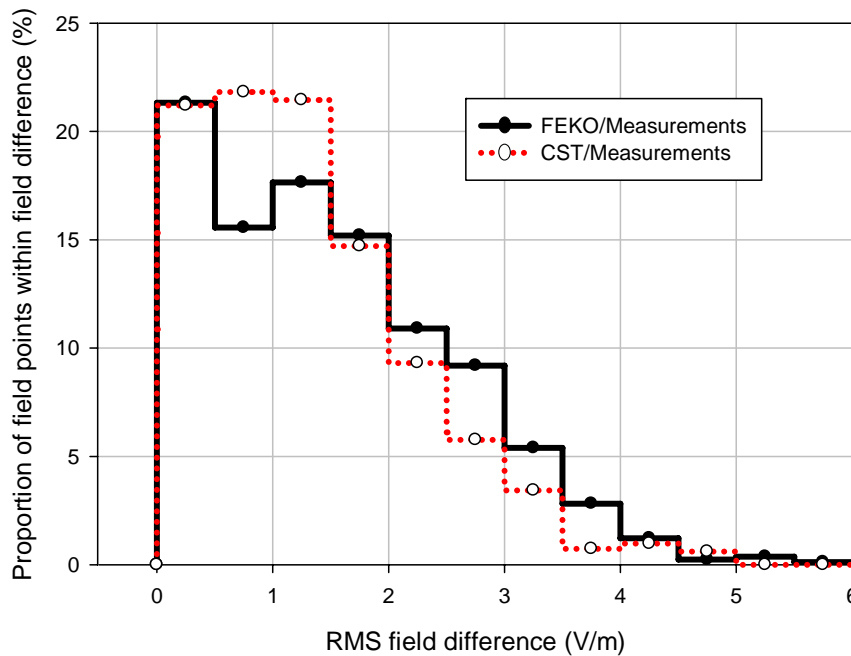


Fig. 5 Comparison of difference between simulated field levels and measurements.

CST average difference = 1.32 V/m, Standard deviation = 0.93

FEKO average difference = 1.52 V/m, Standard deviation = 1.07

Fig. 5 shows histograms of the field differences between the measurements and simulations using CST and FEKO. The histograms are based on total of 3 cut-planes (350,650,950 cm planes) for the empty cavity scenario, with a total of 816 points. For comparison between FEKO and measurements, 21% of points are in the 0-0.5 V/m difference range and 15% in the 0.5-1V/m difference range. For comparison between CST and measurements, 21% of points are in 0-0.5 V/m difference range and 22% in 0.5-1 V/m difference range. It is noted that CST was in better agreement with measurements than FEKO with an average difference of 1.32 V/m compared to 1.52 V/m. The standard deviations were 0.93 and 1.07 respectively.

Further analysis on the effect of the scanning frame can be seen in Fig.6 where the empty cavity was simulated using CST with and without the scanning frame in situ. Measurements were also carried out to verify the results. Fig.7 shows the cavity simulation mesh and the 3 planes of measurement in the cavity. These measurement planes were 950 mm, 650 mm and 350 mm from the bottom of the cavity. These planes are selected such that they are useful for evaluating fields in the head, body and legs of a human seated within a vehicle. 2D cut-planes were extracted from the 3D measurement results to allow a better visualization of the more important cut-planes in this paper. Although 3D scans were performed, it was not practical to scan the entire cavity for all of the different scenarios as each of the measurement planes shown in Fig.7 took 6 hours to scan. The source antenna was on the left hand side window as described in section 3 and hence on the left hand side of the plots. Fig.6 shows the simulation results for 3 planes at 950 mm, 650 mm and 350 mm above the floor of the cavity (see also Fig.9) for a horizontally polarised source antenna. At 950 mm the effects of the scanner frame, which is closest to this plane, are clearly seen from a comparison of the two simulations particularly the fields around the source (lhs). Measurements give a similar field pattern verifying the simulations. At 650 mm the field changes with and without the scanner are small and measurements are in good agreement once more. Further from the scanner frame at 350 mm the field modes for both simulations are not significantly distorted by the scanner and the measured field pattern mode is again in reasonable agreement. It should be pointed out that overall simulations showed that the Z-arm of the scanner had little effect on the cavity fields at 870 MHz. Similar results to those in Fig.6 were found using a vertically polarised source.

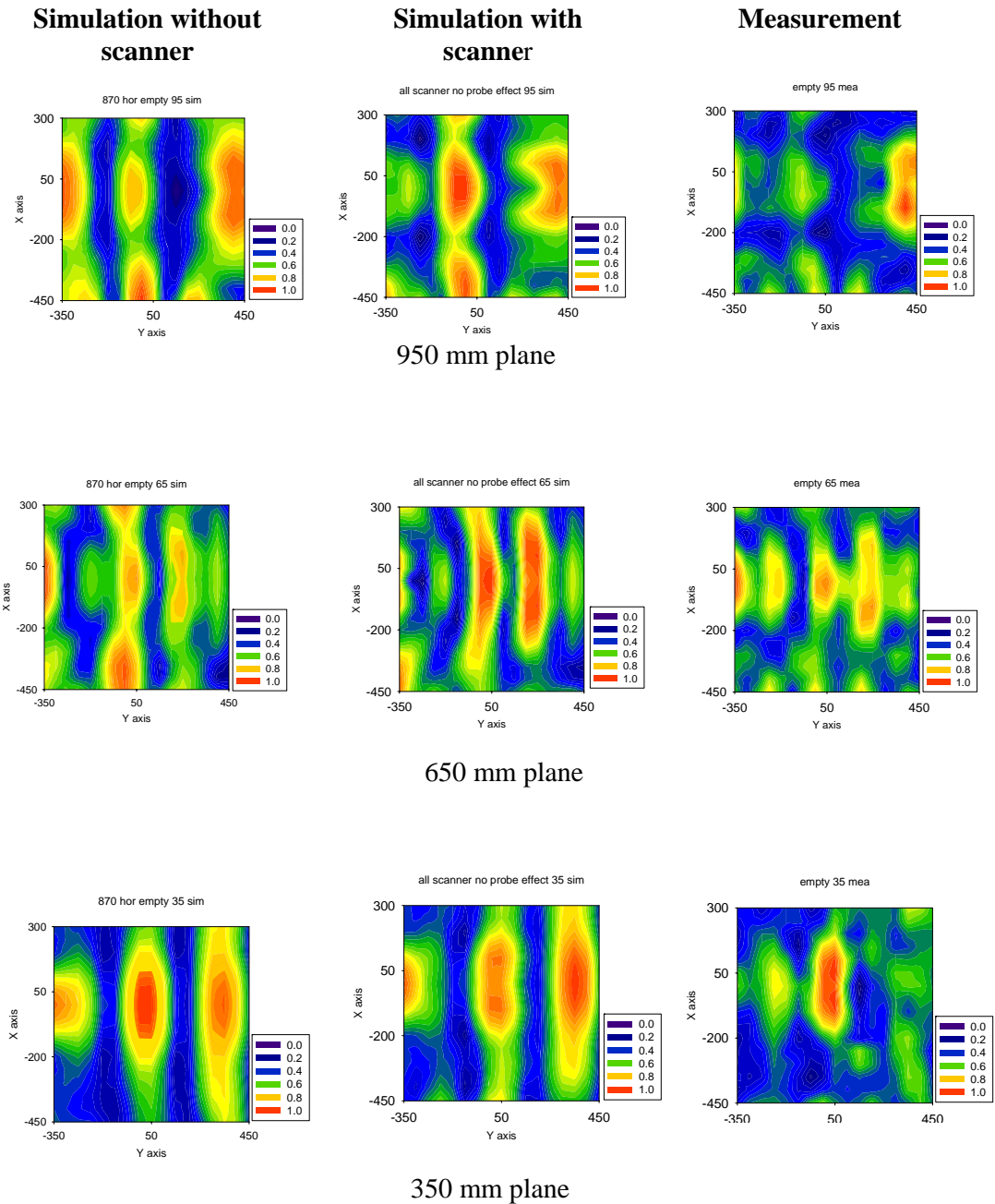


Fig.6 Simulated and measured electromagnetic fields inside cavity with and without scanner (normalised)

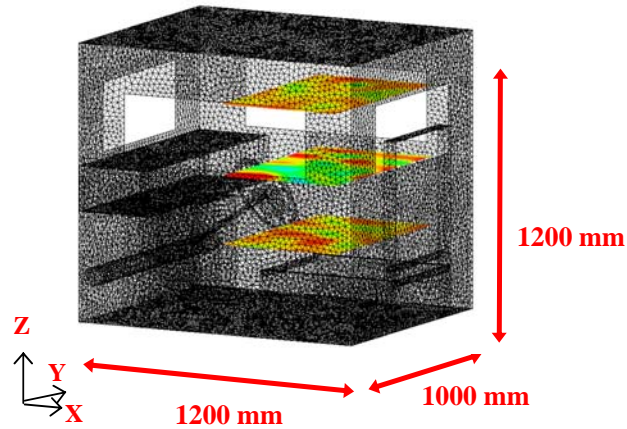


Fig. 7 Cabin model used for field distributions investigation

4. Effects of furnishings on field distributions within vehicle cabin



(a) Seat frame

(b) Steering wheel

(c) Dashboard

Fig. 8 Internal furnishings for cavity

Carefully defined internal furnishings were built for testing in the cavity. Three main components were identified and shown in Fig.8, a seat, dashboard and steering wheel assembly. The steering wheel and seat are constructed from metal and based on actual automotive designed components but without any soft furnishing such as plastic, leather or cloth. Our studies have shown these only have relatively small secondary effects on the electromagnetic fields within this cavity and at this stage an accurate physical model was required for verification. The dashboard was made from Acrylonitrile butadiene styrene

(ABS) in line with common automotive components. Each was a simple mechanical construction to simplify modelling. Fig. 9 shows the measurement set up used to acquire field amplitude data from the cabin model for 3 planes as previously. The scan area is located where the driver and passenger would normally be seated. Each individual item within the cavity (i.e. dashboard, steering wheel and seat) can be easily removed from the model cavity. Field measurement scans were performed within the cavity at 870 MHz with the individual items of furniture installed and with combinations of the three components. The assembly is shown in Fig.9a (rear wall removed) together with a plan view of the area covered by the scan in Fig.9b.

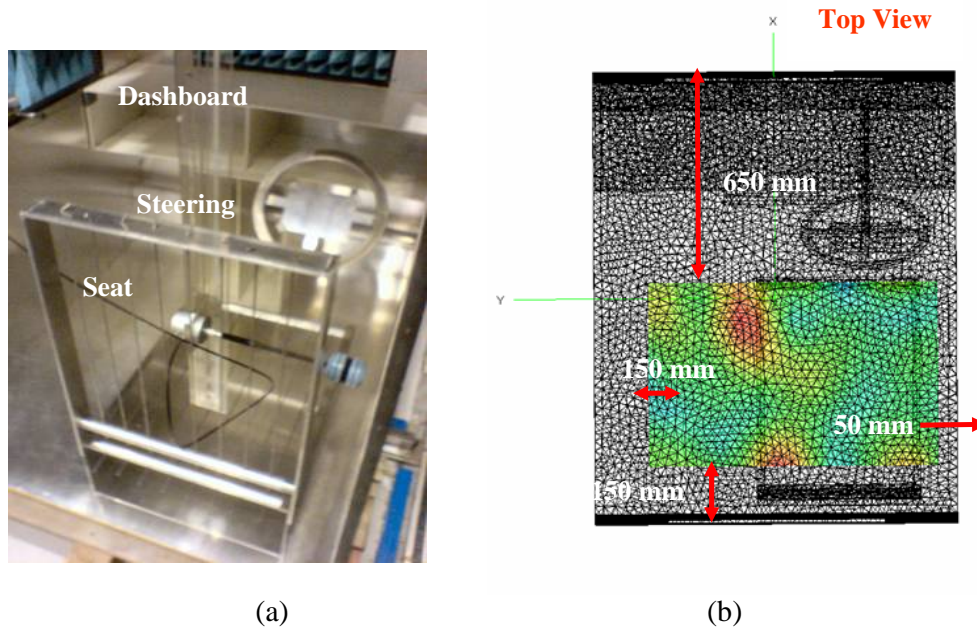


Fig. 9 Experimental setup for field measurements within cavity with furnishings
 (a) Cavity with furnishings (b) Plan view

Changes in field distributions were observed in the entire cavity volume when furnishings were introduced. Some examples of those changes are presented here in Figs 10-13 where the simulated and measured field profiles within the cavity are plotted for scans at 350 mm and 650 mm above the floor. The effect of furnishings would be expected to be most noticeable in these planes as the steering wheel is 330 mm from the cavity base and the seat was 800 mm high with a base 200 mm high. Each part of Figs.10-13 show simulations on the left and measurements in the right hand side. There are 4 rows of measurements – row 1 is the empty cavity; row 2 the cavity with dashboard and steering wheel assembly; row 3 cavity with seat, and finally the cavity with all three furnishings. Only small field level variations were observed when the dashboard made out of ABS plastic was inserted into the cavity and the field profile remained relatively similar. Hence the plots show the effect of the dashboard and steering wheel combined. The other components had a more marked effect.

Inspecting the field plots at 350 mm above the floor and close to the seat base, for horizontal (Fig. 10) and vertical (Fig. 11) polarisations, the following observations can be made. For the empty cavity with vertical polarisation there is a definite field mode generated. For both antenna polarisations there is a clear change in the field patterns when furnishings are

introduced to the cavity. The inclusion of the steering wheel model does not significantly changed the field profile within the cavity for horizontal polarisation, as shown in Fig.10. However there is a significant field redistribution for vertical polarisation where the clear mode structure of the empty cavity has been changed by the steering wheel. When only the seat was included field distributions changed quite significantly - particularly for vertical polarisation, and is likely to be due to the large metal structure scattering the field. Adding all the furnishings produced significant changes in field distribution when compared with the empty cavity for both polarisations. There are fields around the seat base at about 7 V/m and a noticeable high field region to the left of the seat for both polarisations. Fields around the seat for vertical polarisation are less than those for horizontal by about 2 V/m. On comparing simulated and measured fields at 350 mm there was generally good agreement between the field patterns although in some cases levels differed by up to 2 V/m particularly towards the sides of the cavity.

At a height of 650 mm, Figs 12 and 13, the same general observations apply as for the 350 mm plane, there was a redistribution of field modes within the cavity for both polarisations. Again it can be seen that on introducing the steering wheel and seat the field modes changed although overall their effect was less for vertical polarisation than at 350 mm. Overall there was good agreement between simulated and measured field patterns except for the furnished cavity for vertical polarisation where the measured field intensities were higher than simulated levels by up to 2 V/m.

The maximum electric field levels simulated in CST and measured are shown in Table 2 for two antenna polarisations. The agreement for the 350 mm plane was very good and within 0.2 dBV/m while at 650 mm the variation was up to 1.7 dBV/m.

| Plane | Polarisation | CST MWS | Measured |
|--------------|---------------------|----------------|-----------------|
| 650 mm | horizontal | 19.0 dBV/m | 20.4 dBV/m |
| | vertical | 20.6 dBV/m | 19.9 dBV/m |
| 350 mm | horizontal | 20.3 dBV/m | 20.5 dBV/m |
| | vertical | 20.0 dBV/m | 20.1 dBV/m |

Table 2 Maximum electric field levels for cavity with seat, dashboard and steering wheel

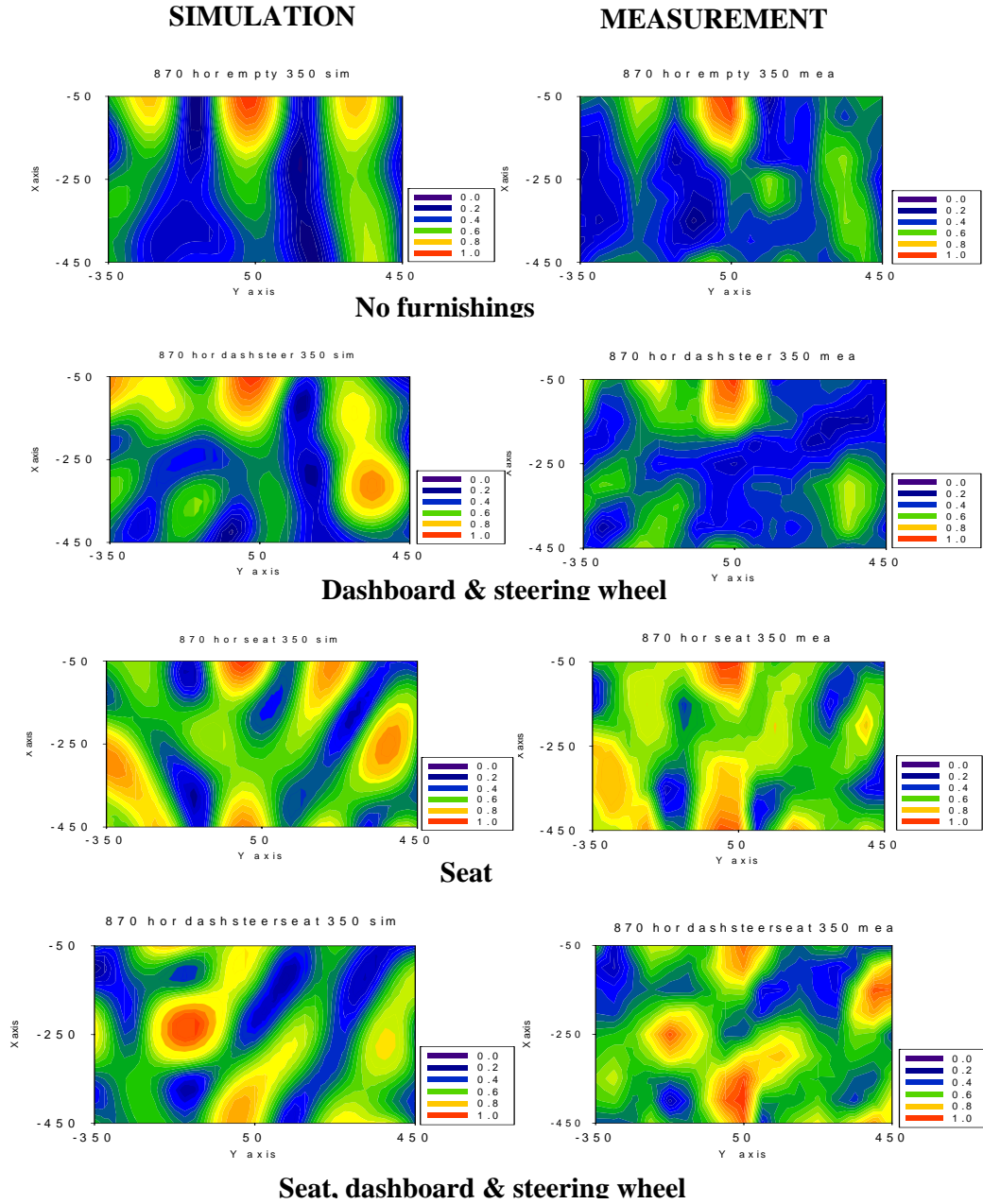
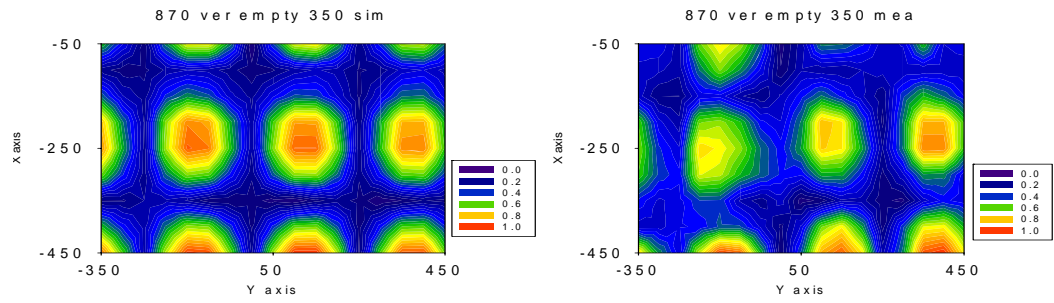


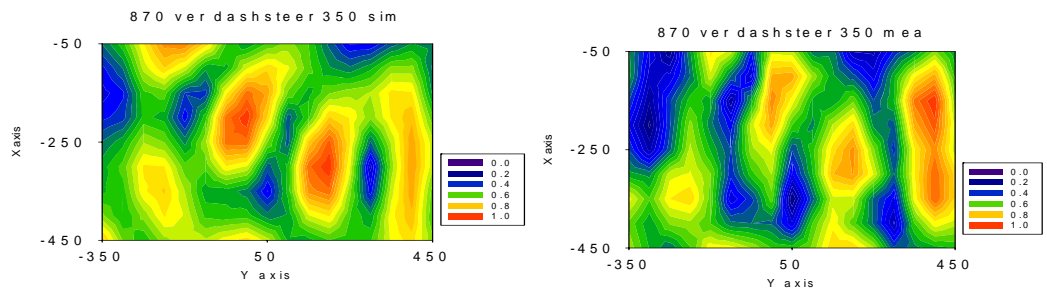
Fig. 10 Field patterns in cavity for 350mm plane
Horizontally polarised source antenna (Normalised)

SIMULATION

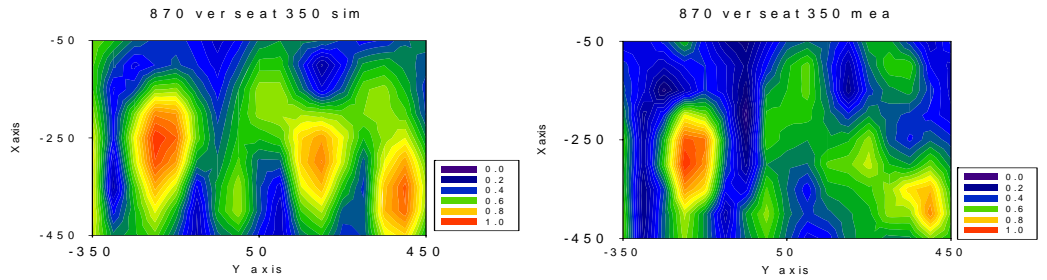
MEASUREMENT



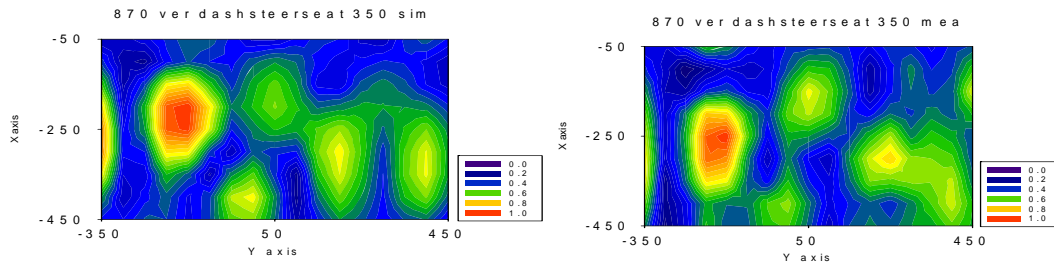
Empty cavity



Dashboard & steering wheel



Seat

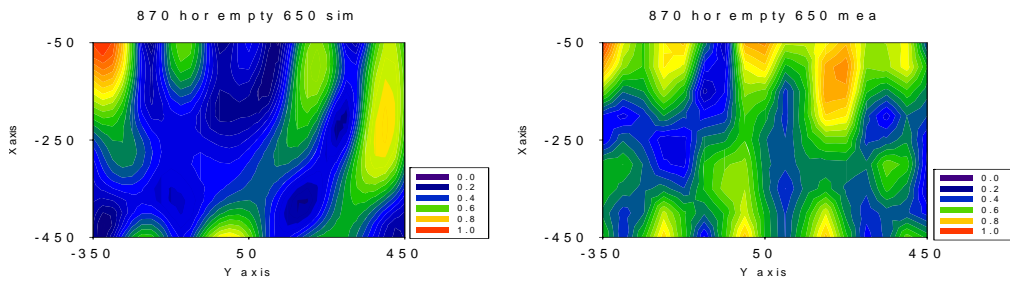


Seat, dashboard & steering wheel

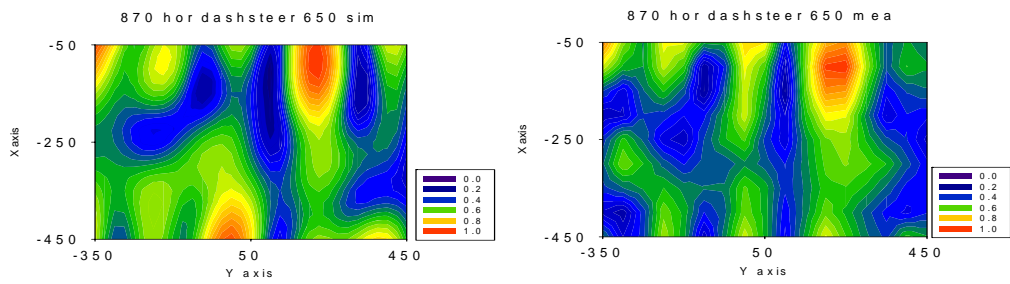
Fig.11 Field patterns in cavity for 350mm plane
Vertically polarised source antenna (Normalised)

SIMULATION

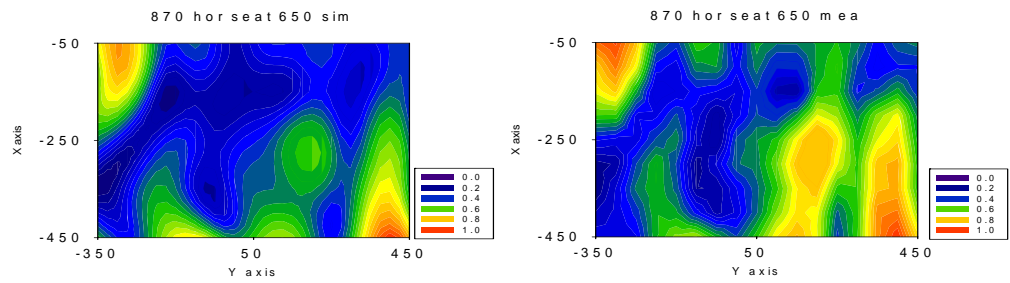
MEASUREMENT



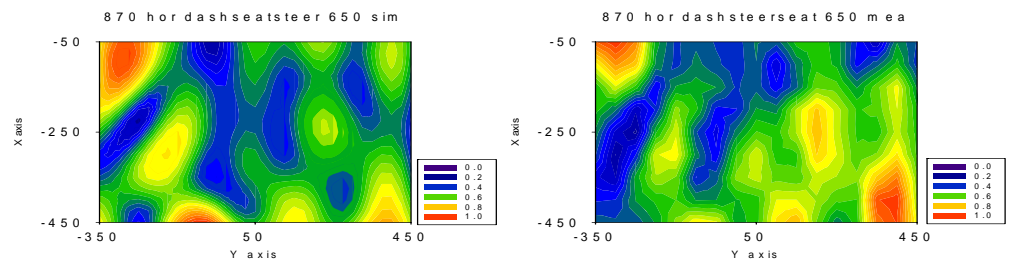
No Furnishings



Dashboard & steering wheel



Seat



Seat, dashboard & steering wheel

Fig.12 Field patterns in cavity for 650mm plane
Horizontally polarised source antenna (Normalised)

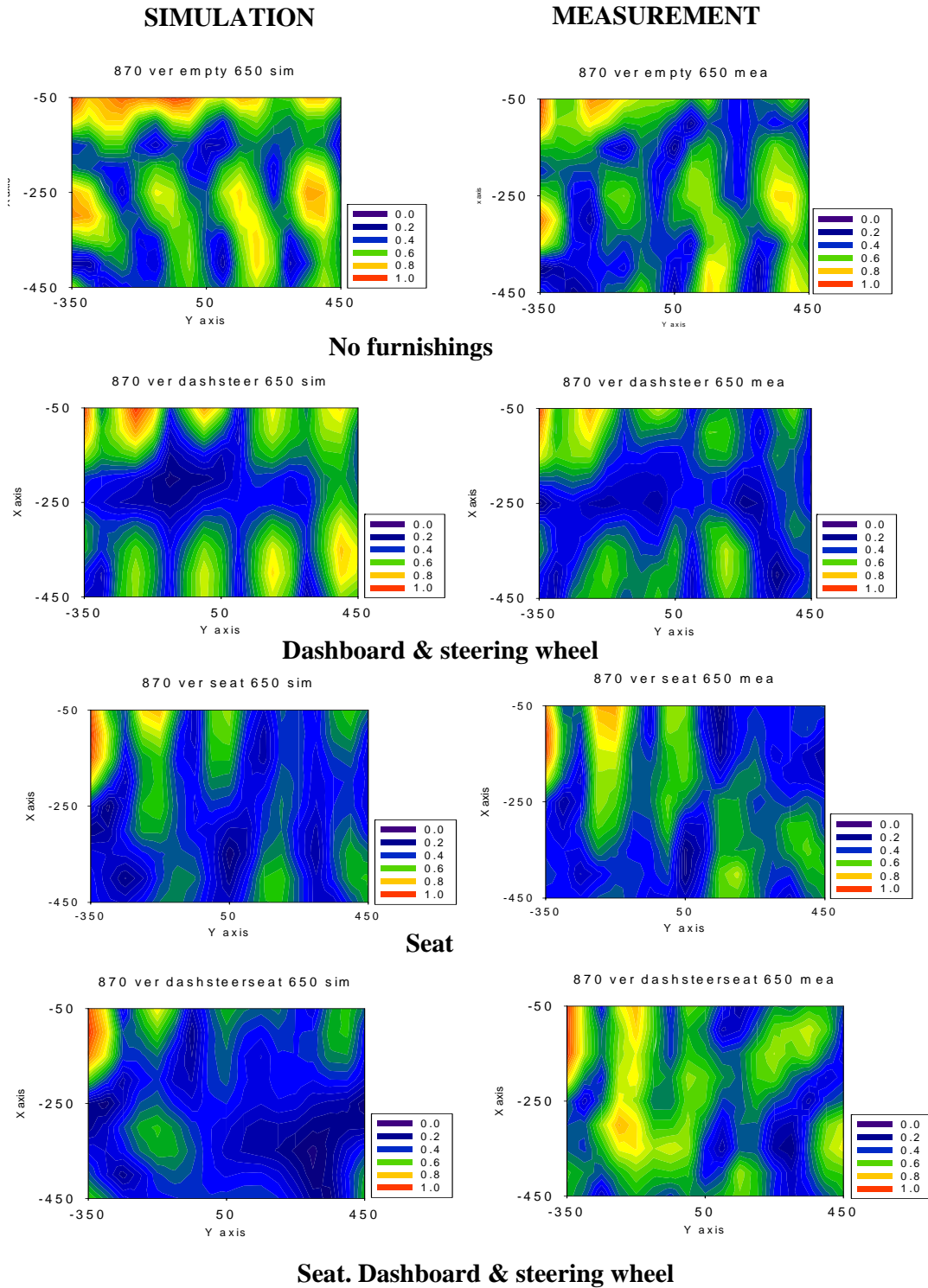


Fig. 13 Field patterns in cavity for 650mm plane
Vertically polarised source antenna (Normalised)

5. Conclusions

A simple cavity model has been used to explore electromagnetic fields generated by an internal source at 870 MHz. It is shown that the introduction of simple furnishings within the cavity causes field distribution variations within the cavity. The most significant field perturbations were caused by the metallic components of the furnishings. These variations have an affect on the performance of on-board transmitters, cause electromagnetic interference to on-board electronic systems and complicate field exposure assessments for human exposure. Measurements of the internal fields were carried out using a 3D scanning frame. Simulations using two electromagnetic software programmes showed that introducing the field measurement scanner into the cavity distorted the internal fields and this was verified experimentally. Further studies showed the effects of introducing simple furnishings into the cavity. Two transmitter polarisations were reported, vertical and horizontal. An ABS dashboard had little affect on the internal EM fields but introducing a metal seat and steering wheel assemblies caused more noticeable field changes. In all cases it was found that the simulated fields were in good agreement with measurements providing confidence in the simulation methods.

This study enhances understanding of complex field behavior within a vehicle. Future work will extend the study to higher frequencies near the 1800 MHz band in this simple cavity. In parallel the fields inside an actual motor vehicle will be computed and measured at the 900 MHz and 1800 MHz bands including full furnishings within the vehicle. The locations of E-field hotspots can be useful to vehicle designers in optimizing the placement location of on-board transmitters and introduce field mitigation techniques in appropriate areas if required.

6. Acknowledgments

The authors wish to thank the DTI and EPSRC for supporting this project. This work is part of the SEFERE project with MIRA as co-ordinator and includes the University of Sheffield, BAE SYSTEMS, Harada Industries, ARUP, Jaguar and Volvo Cars . Visit www.serfere.org for information.

7. References

- [1] ICNIRP, "Guidelines for limiting exposure to time-varying electric, magnetic and electromagnetic fields (up to 300 GHz)," *Health Phys.*, vol. 74, no. 4, pp. 494-522, 1998.
- [2] M. Klingler and A. Lecca, "Comparison between Simulations and measurements of fields created by mounted GSM antenna using a car body instead of an entire vehicle," *Proc. EMC Europe, Barcelona*, pp. 732-742, Sept 2006.
- [3] G. Anzaldi, F. Silva, M. Fernandez, M. Quilex and P. J. Riu, "Initial analysis of SAR from a cell phone inside a vehicle by numerical computation," *IEEE Trans. Biomedical Engineering*, vol 54, no. 5, pp. 921-930, May 2007.
- [4] A. Ruddle, "Validation of predicted 3D electromagnetic field distributions due to vehicle-mounted antennas against 2D external electric field mapping", *IET Science, Measurement & Tech.*, vol.1, no.1, pp. 71-75, Jan 2007.
- [5] D. O. McCoy, D. Zakharia and Q. Balzano, "Field strengths and specific absorption rates in Automotive Environments", *IEEE Trans. Vehicular Tech*, vol. 48, no. 4, pp. 1287-1303, July 1999.

- [6] Y. Shiraki, K. Sugahara, S. Tanabe, K. Nakamoto and T. Watanabe, “Electromagnetic Field Distribution inside an Automobile Vehicle”, IEEE Symposium on EMC 2003, vol. 2, pp 730 – 734, Aug 2003.
- [7] S. Horiuchi, K. Yamada, S. Tanaka, Y. Yamada and N. Michishita, “Comparisons of simulated and measured Electric field distributions in a cabin of a simplified scaled car model”, IEICE Trans. Commun. vol.E90, no. 9, pp. 2408-2415, Sept 2007.
- [8] A. R. Ruddle, X. Ferrieres, J.-P. Parmantier and D.D. Ward, “Experimental validation of time-domain electromagnetic models for field coupling into the interior of a vehicle from a nearby boardband antenna”, IET Science, Measurement & Tech., Vol.1 No.151, No. 6, pp. 430 – 433, Nov. 2004.
- [9] H. Weng, D. G. Beetner, T. H. Hubing, W. Dong and J. McCallum, “Investigation of a Cavity resonance in an Automobile”, IEEE Symposium on EMC 2004, Vol. 3, Pg.766 – 770, 2004.
- [10] S. Savia and R. Langley, “Simulation of Automotive antennas”, Proc. LAPC, Loughborough, Paper no. 53, March 2006.